Tribol Lett (2012) 45:185–194
DOI 10.1007/s11249-011-9870-y

METHODS PAPER

Optical In Situ Micro Tribometer for Analysis of Real Contact Area for Contact Mechanics, Adhesion, and Sliding Experiments

Brandon A. Krick · Jennifer R. Vail · Bo N. J. Persson · W. Gregory Sawyer

Received: 1 July 2011 / Accepted: 26 September 2011 / Published online: 30 October 2011

Abstract An instrument has been developed that allows in situ optical analysis and tribological measurements for contacts between solid bodies; an interferometric optical analysis can be used to measure and observe contact size, contact geometry, near contact topography, tribofilm formation, tribofilm motion, tribofilm thickness, wear debris formation, and wear debris morphology. The optical arrangement is in such a way that a 0th order interference fringe highlights the real contact area of contact, while near contact regions are height-mapped with higher order Newton's rings interference fringes. Images synchronized with force and position measurements allow for the potential to test and validate models for contact mechanics, adhesion, and sliding. The contact and friction measurement between a rough rubber sphere and a polished glass counterface were studied over a range of loads from 1 to 50 mN.

Keywords Contact area · In situ · Optical · Tribometer · Tribology · Contact mechanics · Rubber · Friction

1 Introduction

In situ tribometry is a powerful tool used by materials tribologists to study the interaction between surfaces during contact and sliding [1, 2]. There are various pathways for in situ analysis of a surface. In situ spectroscopies such as Raman spectroscopy have been used to analyze the chemical nature of the interactions by examining the wear surface or transfer films during sliding or just after it exits the contact without changing the environment [3, 4]. In situ electron microscopy is increasingly popular; Varenberg used a scanning electron microscope to analyze the interaction at the interface from the side [5]. Marks showed a liquid-like transfer of gold with in situ transmission electron microscope experiments [6]. The state-of-the-art in in situ tribology was recently reviewed by Sawyer and Wahl [1, 2].

One phenomenon that has been historically probed with in situ techniques is the real area of contact between solids. In situ tribology and contact mechanics experiments are not entirely unprecedented, especially when examining the real contact area between solids [7–13]. Contact area has been indirectly monitored in situ by contact resistance measurements [8, 9] and optical methods of examining the contact through a transparent counter sample [7, 10–16]; Dyson and Hirst examined the real area of contact of metallic films with a phase contrast microscope through a glass disk [7]. Federle used in situ optical techniques to explore contact mechanics and adhesion in the feet of frogs, ants and other insects [14–16]. McCutchen examined the contact area between a polyvinyl chloride surface and an optically transparent counter surface using two optical methods: frustrated total internal reflection and optical interference of the Newton's rings type [10]. The Newton's rings interference can be used to measure contact because the destructive 0th order interference occurs at contact with higher order fringes radiating out in the near contact regions. The higher order fringes can also be used to map the near surface separations, and for closely spaced solids the distribution of interfacial separation, which is of crucial

B. A. Krick · J. R. Vail · B. N. J. Persson · W. G. Sawyer (✉)
Department of Mechanical and Aerospace Engineering, University of Florida, Gainesville, FL 32611, USA
e-mail: wgsawyer@ufl.edu

B. N. J. Persson
IFF, FZ-Jülich, Jülich 52425, Germany

importance for topics such as sealing, mixed lubrication, and the contact heat resistance. These techniques have been used for in situ tribology experiments to explore both film thicknesses and contact geometries [10, 12, 13].

Here, we have designed and constructed a new instrument that uses microtribological probes and methods to perform indentation, friction, and wear experiments while making high fidelity optical interferometric measurements of the contact area. This instrument is capable of measuring normal and friction forces ranging from 10 μN to over 2 N. This design facilitates synchronized measurement of externally applied contact force (including adhesive), friction force, penetration depth, deformation, and in situ optical imaging of the contact with a spatial resolution limited by the diffraction limit. Preliminary optical in situ loading/unloading and sliding experiments were performed between a nitrile rubber half sphere and glass, with the aim to provide experimental measurements that can be compared to the available theories and models on contact area [8, 11, 17–29].

2 Description of the In Situ Optical Micro Tribometer

The in situ optical micro tribometer is capable of performing load/unload, friction, and wear experiments with in situ optical capabilities (Fig. 1). In an experiment, a sample is mounted directly to a load head; the load head measures both normal and frictional forces and is mounted to a piezoelectric stage that displaces the sample toward and away from a counter sample. Beneath the sample and counter sample is a microscope objective facing upward toward the sample; between the sample and objective is a transparent counter sample (in this case a flat optical window). The transparent counter sample is mounted to a piezoelectric stage that generates sliding between the samples. Figure 1 shows a schematic with important components.

A microscope objective (typically 5× or 10×) is mounted beneath the transparent counter sample. The objective has unique, low profile optical path to a 5 mega pixel Sony XCL-5005CR CCD camera. The sample is

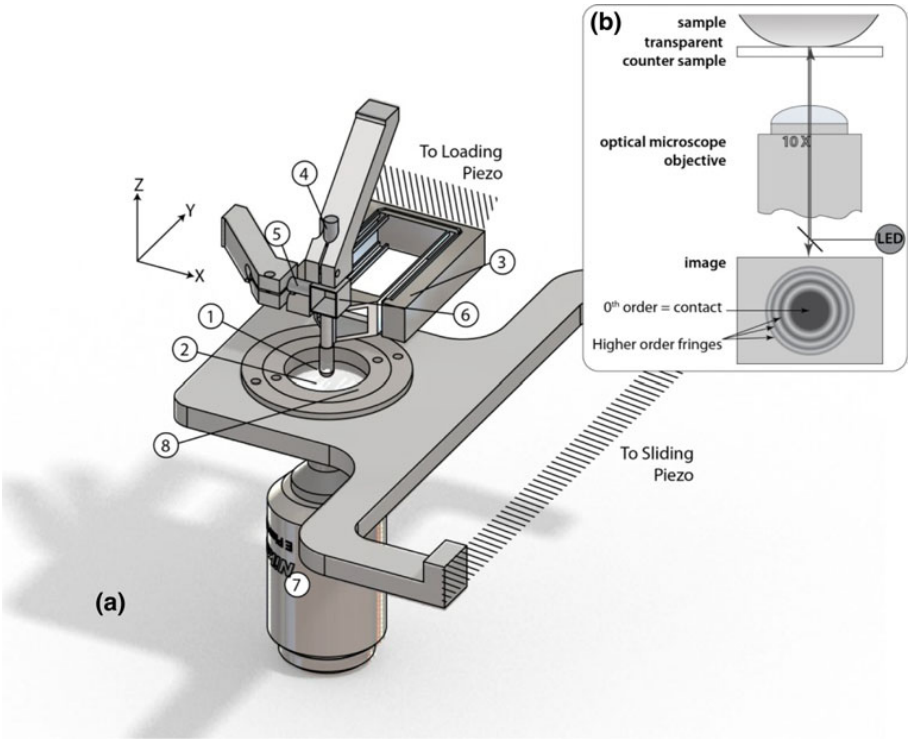

Fig. 1 **a** Schematic of optical in situ micro tribometer: the sample (*1*) is slid against a transparent counter sample (*2*). The sample is mounted directly to a calibrated cantilevered force transducer flexure (*3*). Capacitance probes (*4* and *5*) measure the displacement of a target (*6*) mounted on the cantilevered flexure; with the calibration of the flexure, these displacements provide the normal and friction forces. A microscope objective (*7*) mounted directly beneath the transparent counter sample held by a sample holder (*8*). **b** Schematic of optical pathway. A monochromatic coherent light source passes through the microscope objective and up through the transparent counter sample. The light is reflected off of the surfaces of the sample and counter sample back through the microscope objective and ultimately to a CCD camera. In the image, there is a 0th order destructive interface representing contact and higher order fringes surrounding contact

illuminated through the objective with an interchangeable LED; for this experiment an LED of 595 nm with a measured FWHM of 16 nm was selected.

2.1 Imaging Methodology and Contact Area Analysis

When the sample is lowered into contact with the transparent counter sample a contact area may be observed through interference. At the most basic level, there is a destructive interference fringe of 0th order everywhere the samples are in contact with each other; this allows observation of contact area and geometry (Fig. 1b). In addition to the 0th order fringes, higher order fringes exist when the samples are separated; further information can be determined from the fringes, such as thickness of a film between the solids and relative distance between the solids. The fringe pattern oscillates from dark to light as the separation gap between the samples is increased. The separation distance required for destructive interference (Eq. 1) and constructive interference (Eq. 2) is a function of wavelength, λ, and order.

$$d_{\text{destructive}} = \frac{m}{2}\lambda \tag{1}$$

$$d_{\text{constructive}} = \frac{(2m+1)}{4}\lambda \tag{2}$$

The optical fringe pattern phenomenon is caused by interference between light reflected from the interface between the transparent counter sample and air and the π phase shifted light reflected off of the pin sample.

At a given magnification, the real contact area and geometry is given by the 0th order interference which manifests as a dark area on the digital image for these material sets. Thresholding techniques of the digital image can be applied to calculate this contact area. Unfortunately, additional features such as fringes surrounding the contact and impurities in the glass produce false contact spots in the analysis. To accommodate this error we apply a post processing technique illustrated in Fig. 2. The image that we are analyzing the contact area, image N, is an intensity profile with pixels correlating to contact spots, higher order fringes, background impurities, and a background level intensity (Fig. 2a). Contact is represented by the dark 0th order destructive interference. Surrounding the contact are constructive and destructive interference fringes and other features that are inherent impurities on the glass.

By simply applying a threshold to the image, one cannot accurately separate contact area from the background intensity because the higher order destructive fringes often produce false contact areas. To reduce this error, the image being analyzed is averaged with the image taken directly before and directly after the image of interest. Higher order, non-contact fringes will change as a result of a displacement of the rubber ball toward or away from the optical flat. If there is a change in the separation distance in the near contact zones, then the higher order fringes occupy

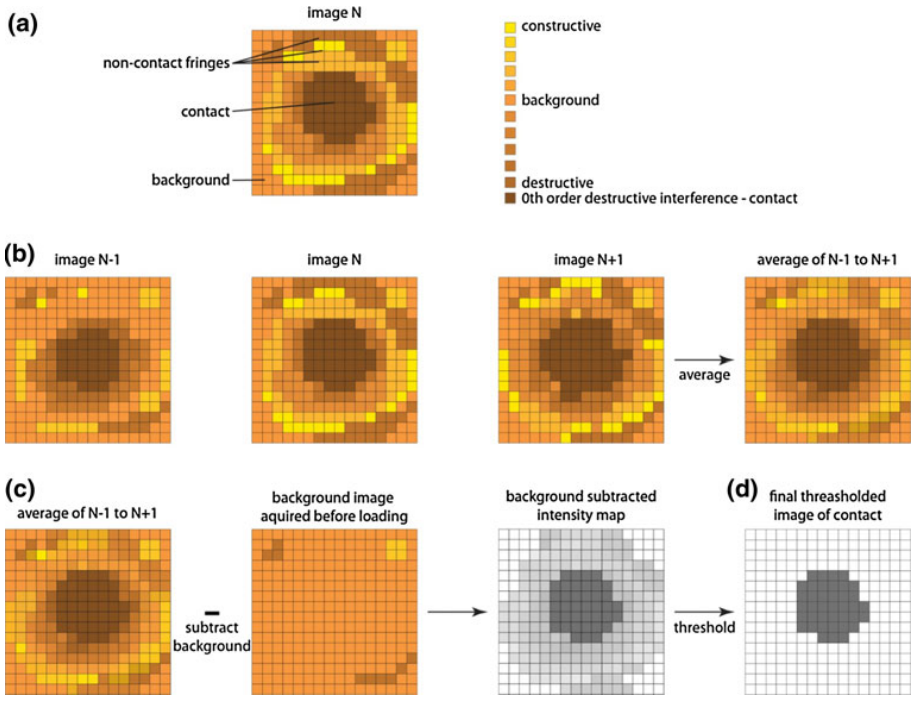

Fig. 2 Post processing technique schematic: **a** image *N* of contact at an applied load. Contact, represented by the dark 0th order destructive interference, is surrounded by constructive and destructive interference fringes and other features that are inherent impurities on the glass. **b** The image being analyzed, the previous image and the next image are averaged to preferentially weight contact and discount higher order fringes. **c** A background image acquired before loading began is subtracted from the averaged image. **d** A threshold is applied to the image revealing the contact area and geometry

different pixels from frame to frame. Consequentially, higher order dark fringes will not overlap throughout the three images as shown in Fig. 2b. This effectively removes higher order fringes, but does not remove impurities in the surface of the glass that result in false contact pixels.

Background impurities are removed by subtracting a background image acquired before loading from the averaged image (Fig. 2c). Finally a threshold can be applied to calculate the contact area (Fig. 2d). This contact area can be calculated by multiplying the number of pixels in contact by the square of the calibration constant 0.35 μm/pixel. The accuracy of the reported contact area is limited by the diffraction limit of light and other optical effects in very thin separations.

2.2 Force Measurements and Positioning Metrology

The load head is responsible for holding the sample, measuring normal and tangential (friction) forces, and applying the normal load by bringing the sample into contact with the counter sample with a piezoelectric stage. It consists of a cantilever that is instrumented with two capacitance probes; one capacitance normal to the contact and one in the sliding direction.

The capacitive probes are aligned with a conductive target that is fixed to the end of the loading cantilever assembly. The probes are calibrated to monitor the change in distance between the capacitance probe and the target that is fixed to the cantilever. The cantilever assemblies consist of two double-leaf cantilevers that are mounted parallel to one another to constrain the flexures to rectilinear displacements. The use of a one double-leaf flexure would result in a change in slope at the capacitive target and would produce adverse effects [30]. The resolution of normal and tangential forces is only limited by the capacitance probe resolution and the stiffness of the interchangeable cantilevers.

Through cantilever selection, normal loads of 2 N or more can be applied for high load cantilevers and normal loads of less than 10 μN can be applied. This particular combination of cantilevers and of capacitive probes can measure forces with uncertainties better than 50 μN and resolution which exceed that by a factor of 10.

Piezoelectric stages are used for both loading displacements and sliding displacements. The piezoelectric stage responsible for bringing the sample into contact and modulating the normal load, the "loading piezo," has a range of 100 μm, resolution of 0.4 nm and repeatability of ±1 nm. The piezoelectric stage that produces the sliding motion, the "lateral piezo," has a range of 1,500 μm, resolution of 3 nm and repeatability of ±14 nm. All of the stages are operated under closed loop positioning control.

Experimental control and acquisition is achieved through LabView. All force and position measurement signals are conditioned externally and interface with LabView with 16 bit analog-to-digital acquisition and control. Force versus displacement measurements are typically taken at 1,000 samples per second. Images are also acquired with LabView and are time-synched with all force and position data at as quickly as 15 frames per seconds.

3 Materials

Commercially available Buna-N nitrile rubber spheres of 4.8 mm diameter were used in this study. The Buna-N rubber has a supplier specified durometer of 70A corresponding to a modulus of approximately 5.5 MPa. The spheres were cut in half with a razor blade and attached to the end of the cantilever. Prior to experiments, the half sphere was characterized with a Veeco Dektak 8 Advanced stylus profilometer, a Veeco Wyko NT9100 scanning white light interferometer (Fig. 3a–c), and an ASYLUM MFP-3D atomic force microscope; the measured RMS roughness of the rubber spheres was 5.2 μm. The surface roughness power spectrum was determined from this characterization (Fig. 3d) [29] and the resulting fractal dimension is $D_f \sim 2$.

A borosilicate float glass optical window was used as the transparent counter sample. The windows were 25 mm in diameter and 3 mm thick. The manufacturer specified modulus of the glass is four orders of magnitude higher than the rubber sample at approximately 64 GPa. The glass samples have RMS roughness of 2.06 nm measured with the stylus profilometer; that is more than three orders of magnitude less than the roughness of the rubber. These large differences in roughness and modulus make the glass appear infinitely stiff and perfectly smooth when compared to the rubber sample.

4 Description of Loading and Sliding Experiments

For these experiments, a 2.4 mm radius nitrile rubber half sphere was pressed against and slid against borosilicate glass windows. The nitrile spherical cap was brought into contact with the glass window to a prescribed force; the piezo was commanded to move at a constant rate of 2.75 μm/s during loading and unloading. Four different experiments were run with target loads of 5, 10, 25, and 50 mN. Images were acquired at half second intervals and were synchronized with the experiments; these digital images were then processed to compute the measured real contact area.

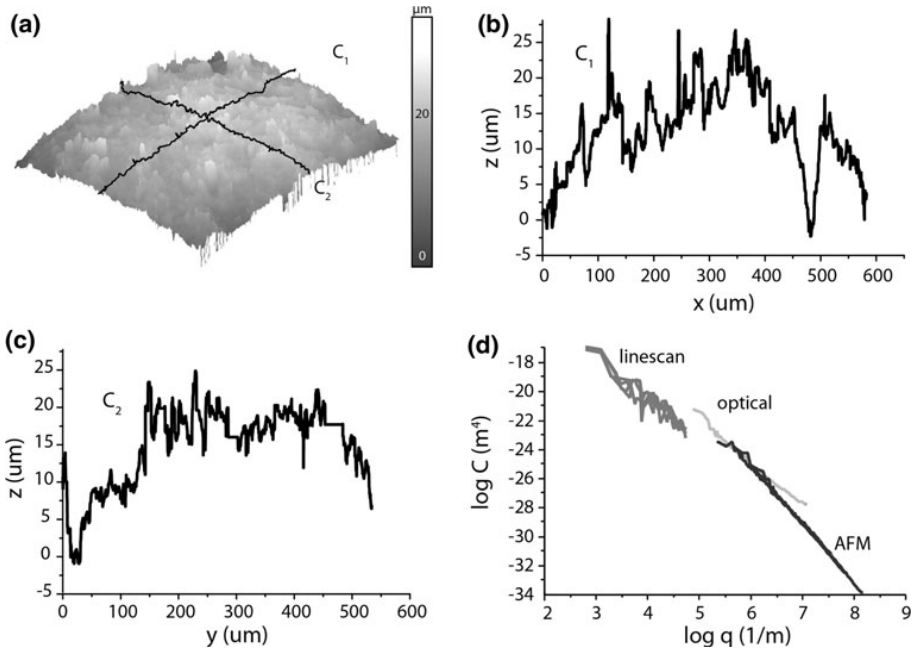

Fig. 3 Surface profilometry of nitrile spherical cap 2.4 mm radius. **a** Surface profile acquired from a Veeko Wyko NT9100 Scanning White Light Interferometer. **b** and **c** line scans taken across sample indicated by C_1 and C_2. **d** Surface roughness power spectrum of nitrile ball. The fractal exponent of the surface is 1.8; this determined by the slope of the log C versus log q relationship

Linear reciprocating sliding experiments were performed on the nitrile half sphere. For each test, the sample was brought into contact at the desired normal force loading: 25 and 50 mN; a static image was acquired before the onset of sliding. Sliding experiments were performed at sliding velocities of 20 and 50 μm/s over a stroke of 800 μm; images of the contact were acquired before and during sliding. Images were acquired at six frames per second.

5 Results and Discussion

Figure 4 shows the contact area as a function of externally applied normal load for nitrile rubber half spheres, where each data point represents a processed image file. There is a nearly linear increase in contact area with increasing force over the range of the experiments, as predicted by contact mechanics theories (see, e.g., Ref. [28]), as long as the area of contact, A, is small compared to the nominal contact area A_O. This linearity means that the (average) pressure is the area of real contact is nearly constant.

In all cases, there is a strong hysteresis in the contact area plotted against externally applied force in the loading versus unloading of the rubber against the glass. This has been explained by considering the loading scenario as a crack closing between the rubber and the glass, and the unloading and breaking of contact as a crack opening: At a distance r away from the tip of a propagating crack the rubber experiences time-dependent deformation characterized by a frequency υ/r, where υ is the crack tip velocity.

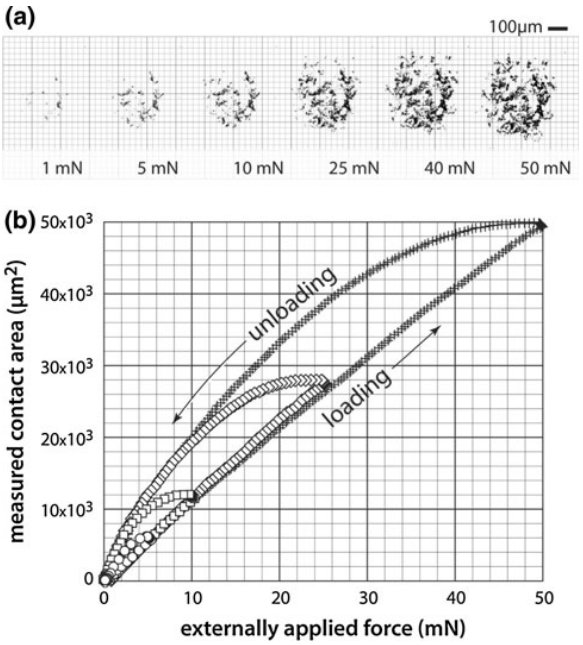

Fig. 4 Measured real contact area versus externally applied force of the nitrile spherical cap pressed against the borosilicate glass window. **a** Processed contact area images for loadings of 1, 5, 10, 25, 40, and 50 mN. **b** Contact area plotted against externally applied force for four loading and unloading profiles

Rubber-like materials are viscoelastic, and a large energy dissipation in the rubber may occur at a distance r from the crack tip where the perturbing frequency υ/r is close to the frequency where $\tan\delta = \mathrm{Im}E/\mathrm{Re}E$ is maximal. For a fast

DOCKET ALARM

Explore Litigation Insights

Docket Alarm provides insights to develop a more informed litigation strategy and the peace of mind of knowing you're on top of things.

Real-Time Litigation Alerts

Keep your litigation team up-to-date with **real-time alerts** and advanced team management tools built for the enterprise, all while greatly reducing PACER spend.

Our comprehensive service means we can handle Federal, State, and Administrative courts across the country.

Advanced Docket Research

With over 230 million records, Docket Alarm's cloud-native docket research platform finds what other services can't. Coverage includes Federal, State, plus PTAB, TTAB, ITC and NLRB decisions, all in one place.

Identify arguments that have been successful in the past with full text, pinpoint searching. Link to case law cited within any court document via Fastcase.

Analytics At Your Fingertips

Learn what happened the last time a particular judge, opposing counsel or company faced cases similar to yours.

Advanced out-of-the-box PTAB and TTAB analytics are always at your fingertips.

API

Docket Alarm offers a powerful API (application programming interface) to developers that want to integrate case filings into their apps.

LAW FIRMS
Build custom dashboards for your attorneys and clients with live data direct from the court.

Automate many repetitive legal tasks like conflict checks, document management, and marketing.

FINANCIAL INSTITUTIONS
Litigation and bankruptcy checks for companies and debtors.

E-DISCOVERY AND LEGAL VENDORS
Sync your system to PACER to automate legal marketing.